Available online at www.sciencedirect.com
ScienceDirect
Journal of Sound and Vibration 311 (2008) 74–96
JOURNAL OF SOUND AND VIBRATION
www.elsevier.com/locate/jsvi

On dry friction modelling and simulation in kinematically excited oscillatory systems

George Juraj Stein*, Radúz Zahoranský[1], Peter Múčka[2]

Institute of Materials and Machine Mechanics, Slovak Academy of Sciences, Račianska 75, SK-831 02 Bratislava 3, Slovak Republic

Received 18 January 2007; received in revised form 21 August 2007; accepted 22 August 2007
Available online 24 October 2007

Abstract

This paper deals with the analysis and simulation of a general single degree of freedom (sdof) oscillatory system with idealised linear viscous damper and dry friction. For dry friction modelling the phenomenological macro-slip approach is employed, described in mathematical form either by the signum function approach or by the physically correct stick–slip approach assuming switching phenomena on a short time scale. Both approaches are illustrated first using a steady-state harmonic acceleration excitation with constant amplitude and then a stationary random acceleration excitation, corresponding to a field-measured excitation in a vehicle. The differences in the two approaches are highlighted, indicating that the physically correct stick–slip approach describes the friction phenomenon better than the standard signum approach. The signum approach is prone to false numerical oscillations completely distorting the acceleration response signal in comparison to measured suspension system response. The acceleration transmissibility response is analysed in respect to the dry friction force magnitude, employing stationary random excitation. A sdof oscillatory system without viscous damping, subjected to both stationary random acceleration and harmonic acceleration is analysed, too. It is shown that such a system can be used without serious practical problems; however, no implications on its performance from the analysis under harmonic constant amplitude acceleration excitation can be made.

1. Introduction

The analysis of translatory oscillatory systems is an essential part of machine dynamics and the starting point of further studies in engineering vibrations. The essential form of such an oscillator is a combination of mass m, linear mass-less spring with spring constant k_x and an idealised viscous damper with resistance proportional to the relative velocity, described by the damping constant b as schematically illustrated in Fig. 1a. The mathematical treatment of such a system is well known—it is described by a linear second-order ordinary differential equation with constant, time-invariant coefficients. This equation has to be solved for the mass m absolute displacement variable x and its time derivatives $\dot{x}$, $\ddot{x}$ for given initial conditions and imposed excitation acting in the direction of free system movement (for systems illustrated in Fig. 1 in the horizontal

*Corresponding author. Tel.: +4212 5930 9422; fax: +4212 5477 2909.
E-mail addresses: stein@savba.sk (G.J. Stein), ummszaho@savba.sk (R. Zahoranský), ummsmuc@savba.sk (P. Múčka).
[1]Tel.: +4212 5930 9404; fax: +4212 5477 2909.
[2]Tel.: +4212 5930 9402; fax: +4212 5477 2909.

0022-460X/$ - see front matter
doi:10.1016/j.jsv.2007.08.017

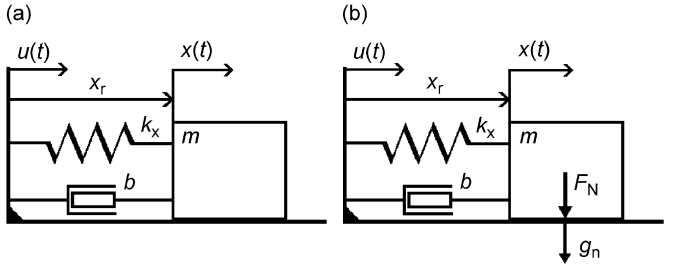

Fig. 1. Schematic layout of the analysed horizontal single degree-of-freedom oscillatory system: (a) a frictionless oscillatory system and (b) the same horizontal system including dry friction.

direction). The external excitation can be either a time variable force $F(t)$ acting on the mass m or a kinematic excitation in form of absolute displacement $u(t)$ and its derivatives $\dot{u}(t)$ or $\ddot{u}(t)$ acting on the oscillatory system support, as is the case analysed here. The equation of motion is then

$$m\ddot{x} + k_x(x-u) + b(\dot{x}-\dot{u}) = 0 \tag{1}$$

which can be re-written using the time-dependant relative displacement $x_r = x-u$ and its time derivatives $\dot{x}_r$, $\ddot{x}_r$ as

$$m\ddot{x}_r + k_x x_r + b\dot{x}_r = -m\ddot{u}. \tag{2}$$

However, for many real-world mechanical oscillatory systems this description is too simple:

- Structural constraints limit the free travel, i.e. stroke (relative displacement x_r) of the oscillating mass.
- Direction of movement is restrained by some sort of guiding mechanism.
- Description of vibratory energy dissipation by a linear, relative velocity-dependant damper is too simple.

Another important issue is the dry friction, ever-present in any mechanical system. The friction element may be introduced intentionally, to act as the means of vibratory energy dissipation, or more likely, is an unwanted consequence of the system design or construction. In such oscillatory systems the influence of friction cannot be neglected [1]. The description by the linear single degree of freedom (sdof) oscillatory system may be an oversimplification of reality and its analysis may lead to erroneous conclusions. This is specially so for random kinematic excitation, as is often the case in ground transportation. In this class of problems the variable of interest is the vibratory acceleration $\ddot{x}$ of mass m rather than the displacement variables. Hence, it is worthwhile to analyse oscillatory systems in which both a linear damper and a friction element (described by a general friction force F_f) are present, as depicted schematically in Fig. 1b, especially from the point of view of the acceleration transmissibility. Then the above-mentioned equations of motion are slightly modified to become:

$$m\ddot{x} + k_x(x-u) + b(\dot{x}-\dot{u}) + F_f\,\mathrm{sgn}(\dot{x}-\dot{u}) = 0, \tag{3}$$

or

$$m\ddot{x}_r + k_x x_r + b\dot{x}_r + F_f \mathrm{sgn}(\dot{x}_r) = -m\ddot{u}. \tag{4}$$

The general damping force F_d (or mixed damping force in DenHartog's notation [2]) is described by expression:

$$F_d = b(\dot{x}-\dot{u}) + F_f\,\mathrm{sgn}(\dot{x}-\dot{u}) = b\dot{x}_r + F_f\,\mathrm{sgn}(\dot{x}_r), \tag{5}$$

where $(\dot{x}-\dot{u}) = \dot{x}_r \equiv v_r$ is the relative velocity between the sliding surfaces.

From a mathematical point of view such an oscillatory system belongs to the class of non-conservative, nonlinear oscillatory systems. Nonlinear oscillatory systems can be classified by various criteria, such as:

- Oscillatory systems with continuous type of nonlinearity (smooth systems). The mathematical solution is essentially time-invariant and can be treated by sophisticated analytical methods.

- Oscillatory systems with discontinuous type of nonlinearity (dry friction, impacts, free-play, etc.), as is the case here. The discontinuous non-smooth nonlinearity causes a time-dependant change in the system dynamics [3]. The mathematical solution relies essentially either on the use of a non-smooth discontinuous function, dependant on a system variable, or on the use of a control variable, for switching between solutions, respecting the change in system dynamics on a short time scale [4,5]. The solution poses some mathematical difficulties, especially when real-world time data, sampled at periodic instants of time, have to be compared with the simulation results, as was the case here. Common stiff differential equations solvers with variable time step are sometimes not suitable, so other robust methods have to be used.

The most common approximate analytical approaches are either to use the harmonic balance method, described first in this context fully by Den Hartog [2], or to solve the particular differential equations in respective time intervals [6–9], which is laborious. Here the simulation approach will be followed, assuming excitation by vibratory acceleration $\ddot{u}(t)$, to arrive at solutions that are both viable from the engineering point of view and realisable by any commercially available simulation software. The aim was to obtain simulation results (response time courses) which are very close to those measured in the field operating conditions. This, together with some numerical signal characteristics, was the ultimate measure of model acceptability.

There are not many recent papers dealing with base excitation of an oscillatory system with both dry friction and viscous damping, known to the authors, exceptions being [10,11]. There is a paper indicating exploration of practical viability of semi-active dry friction damping in the automobile suspension [12]; however, no further results have been published since. Most of the approaches treated in the literature have the objective of obtaining closed-form solution for harmonic excitation [7,9]. Such an approach may be well justified for advanced analysis of nonlinear systems; however, it brings little information that is directly applicable for many practically oriented tasks. Out of papers dealing with the base excited systems Hundal [10] is concerned with analytical solutions in the frequency band $(0, 2 \times f_0)$, where f_0 is the system natural frequency. He derives conditions governing the transition between the continuous motion and the motion with two stops within each cycle. He concludes that his results are identical for this case with those obtained by Den Hartog [2]. Schlesinger [11] treats a more complicated system, which describes more realistically a suspension system. He is concerned mainly with the system transmissibility and particularly with the relative displacement transmissibility around resonance in relation to the system structure and value of the dry friction, and suggests ways to reduce the relative displacement. He indicates: ''care must be taken in interpreting these transmissibility curves if the requirement is to reduce acceleration of the supported mass''. He concludes, without going into explanatory details, that ''the acceleration isolation can thus be expected to be better than the displacement isolation shown'', which may be a gross oversimplification.

The most important fundamental theoretical work concerning harmonic excitation was probably that undertaken by Den Hartog [2] and his findings are widely quoted since. His calculations are supported by experiments; however, made on a rotary system. It is interesting to note that thereafter the case of mixed damping is not mentioned at all in the subsequent textbooks [6,13,14].

The treated topic is a specific, rather simple, contact mechanics problem. More details on mathematical treatment of more general contact mechanics problems are given in Ref. [15], which is a part of a highly reputed series on this important mechano-mathematical problem.

In analysing an oscillatory system with both viscous damper and dry friction the primary question concerns the relative contribution of both dissipative terms to the total vibratory energy dissipation and then the influence of both terms on the typical system response characteristics, e.g. transfer function, time response, etc. Also of interest is the ratio between the friction force and the mass m inertial force while sticking (to be described latter). This will be the aim of this paper. One method of those mentioned above, which would describe the particular case the best, has to be selected and implemented in the simplest and easiest way, while still accounting for all the major problem features. This paper may assist in comparing simulation methods applicable to the case described, and in selection of the most appropriate one for modelling response to the realistic low-intensity random acceleration excitation.

Applications assuming random kinematic excitation in transport industries are reported by Rakheja et al. [16] and by Gunston [17]. In a recent work of Gunston et al. [18] the MATLAB/Simulink® was used. It was

concluded that the built-in signum function approach was not satisfactory and a different approach had to be followed using a more sophisticated switching algorithm.

2. Dry friction models

The first comprehensive scientific work on the dry friction is attributed to Coulomb in 1785; however, already around 1500 the universal genius Leonardo da Vinci was occupied by the research of dry friction [19]. Despite many years of research, the mathematical description of this phenomenon is not yet fully developed [1,19]. The phenomenon is not always reproducible, as its extent depends on surface state, lubrication, asperities, temperature, magnitude of normal force, relative velocity, etc. [1,13,19,20].

Various approaches to this problem are presented in the literature, e.g. [21]:

- The macro- (or phenomenological) approach assumes a single dissipative force acting at the interface between the sliding surfaces. This approach is often described as a static friction model. One of a more recent model is that one based on a generalised hysteretic operator model, which enables to include both the nonlinear stiffness and friction into the damping element description [22,23]. This is the generalisation of the older Dahl model. This model, as well as the Masing element, together with the Bouc–Wen models are often used for analysis of oscillatory systems with nonlinearity and hysteresis, as illustrated, for example, in a recent paper [24].
- The micro-approach takes into account detailed knowledge of characteristics of the sliding surfaces including roughness, asperities, adhesive phenomena, friction hysteresis, limit cycles, surface lubrication, other tribological parameters, etc. This approach is often used in the so-called dynamic models. Some of the models that have been hitherto developed include, for example, the LuGre model, the Leuven model and the Petrov–Ewins model [1,13,20]. Many more models exist in the literature [15,22,23]. All these models have in common the assumption of a detailed knowledge of the phenomena associated with the sliding surfaces. The describing differential equations are nonlinear and complicated and their use requires knowledge of numerical values of a number of descriptive parameters that have to be established by measurement under controllable conditions. As a result, it is not practicable to use this approach for applications in the transport industry with its multitude of operating conditions, loading, environmental influences, etc. These models are mentioned here for the sake of completeness.

Static friction models are based on a simple relation of the friction force F_f to the relative velocity v_r between the sliding surfaces in a phenomenological way. Four basic approaches, according to the notation in Fig. 2, are described below:

(A) The common Coulomb-type friction characteristics—F_{fk}, which may be mathematically described by the relay characteristics [1,21,25]:

$$F_f = F_C \mathrm{sgn}(v_r), \quad F_C = F_{fk} = \mu_k F_N, \tag{6}$$

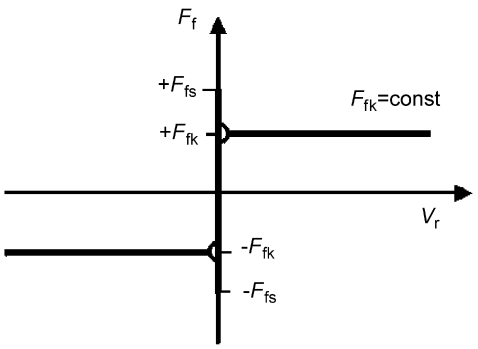

Fig. 2. Friction force F_f courses as function of the relative velocity v_r.

where F_f is the friction force course, F_C is the Coulomb friction force. This model involves the proportional relationship between the Coulomb friction force F_C, sometimes denoted as kinetic friction force F_{fk}, and the normal loading force F_N [13,14] which is usually assumed to be constant. The proportionality constant μ_k is the dimension-less kinetic friction coefficient, introduced by Euler around 1765 [19]. The kinetic friction force F_{fk}, is independent of v_r; however for $v_r = 0$ it cannot be determined, i.e. the force F_f can have any value in interval $(-F_{fk},\ +F_{fk})$.

The signum function $\mathrm{sgn}(v_r)$ (or $\mathrm{sign}(v_r)$ in some literature) is often [6,8,14,25] mathematically described as

$$\mathrm{sgn}(v_r) = \begin{cases} +1 \text{ for } v_r > 0, \\ -1 \text{ for } v_r < 0. \end{cases} \tag{7}$$

However, different authors define different function values for the argument value $v_r = 0$ [3,6,26]. Note also that the signum function, as defined by expression (7) has no limit for $v_r = 0$ and is therefore not differentiable for $v_r = 0$, and hence is not a smooth continuous function.

(B) In reality a larger force is needed to start the sliding motion, i.e. for overcoming the adhesion at zero relative velocity a larger force F_{fs} is required than when the two surfaces are continuously sliding over each other [13,14]. The friction force at $v_r = 0$ has to be described as a function of a limit force F_L, external to the dry friction interface. The limit force F_L is obtained by analysing the force balance across the interface between the sliding surfaces, and has to be compared to the static friction force value F_{fs}:

$$\text{if } |F_L| \leqslant F_{fs} \Rightarrow v_r = 0. \tag{8}$$

If this condition is met the system is at standstill in the so-called stick state, indicated in Fig. 2 by the vertical line segment. If at a certain time instant the adhesion force F_{fs} is overcome by the external force, the oscillatory systems starts to move abruptly and the relative velocity v_r attains some non-zero value. Eq. (6) is valid from this instant until v_r eventually decreases to zero and the system stops again for a certain time interval until the static friction force is overcome again. This start-slide-stop movement (stick–slip movement) leads to a non-unique solution of equations describing the motion and poses mathematical difficulties [8,14,25,26]. In analogy to the above, the static friction coefficient μ_s is defined as $\mu_s = F_{fs}/F_N$, and $\mu_s > \mu_k$, because $F_{fs} > F_{fk}$.

(C) Any technical oscillatory system has a limitation on its stroke (relative displacement amplitude x_{ra}) due to the structure design features, defined as a maximal value x_{rM}. If at any time instant $x_{ra} \geqslant x_{rM}$ the structure is hit hard an impact with high acceleration peaks would occur leading to a possible chaotic behaviour and an excessive structure loading. In practical systems measures are taken to avoid this situation and soften the end-stop impact however in this analysis the validity of all formulas will simply be tested against this constraint without going into a detailed analysis of the influence of the end-stops. Details on the influence of the end-stops can be found, e.g. in Ref. [27].

(D) In some cases of well-lubricated surfaces the sliding friction force is also dependant on relative velocity. It exhibits a certain minimum at a relative velocity known as the Stribeck's velocity v_S and then increases with higher velocities. It is described by a velocity-dependant function $f(v_r)$:

$$\begin{aligned} F_f &= f(v_r) && \text{if } v_r \neq 0, \\ F_f &= F_L && \text{if } v_r = 0 \text{ and } F_L < |F_{fs}|, \\ F_f &= F_{fs}\,\mathrm{sgn}(F_L) && \text{if } v_r = 0 \text{ and } F_L \geqslant |F_{fs}|. \end{aligned}$$

In some simulation approaches the Stribeck's effect is modelled using a Gaussian distribution function [28] to account for the discontinuous natural dynamics of the change of the state at the start of the slipping motion (step transition $F_{fs} \to F_{fk}$ or $\mu_s \to \mu_k$). It is argued, that the restraining (adhesive) force is a composition of all the micro-actions across the interface of contacting surfaces and their asperities [4,20]. Obviously these actions take place consecutively and not abruptly. The Gaussian model introduced by Eq. (10) is a reasonable continuous approximation of this state change:

$$F_f = \left| F_{fk} + (F_{fs} - F_{fk})\,\exp\left\{ -\left(\frac{v_r}{v_S}\right)^2 \right\} \right| \mathrm{sgn}(v_r), \text{ for } v_r \neq 0. \tag{10}$$

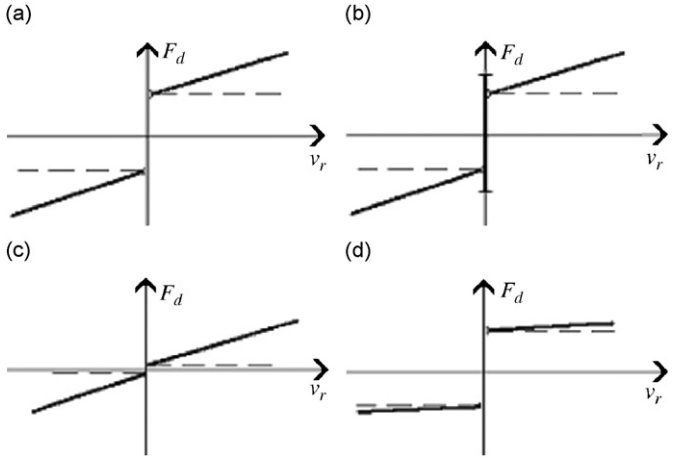

Fig. 3. Illustration of the damping force F_d (——) dependence on the relative velocity v_r, the Coulomb friction force (— —): (a) general case without adhesive friction; (b) general case with adhesive friction; (c) friction influence negligible; and (d) viscous damping negligible.

As indicated before, further analysis will deal with an oscillatory system assuming two ways of dissipating vibratory energy—by a linear viscous damping term and by a dry friction term—Eq. (5). Four different cases may arise, illustrated in Fig. 3, representing the respective proportion of each dissipating term according to the dependence of the general damping force F_d on the relative velocity v_r.

Obviously, if the friction influence is negligible, e.g. good lubrication can be assumed or the force acting on the body to be isolated is much larger than that one due to friction, the respective term can be neglected and the sdof theory fully applies—case of Fig. 3c. The case of Fig. 3d is treated analytically at length in the literature [2,6,13,14] and will be used as a starting point of the problem analysis.

3. Approaches to the dry friction analysis and modelling

3.1. Introduction

By employing static friction models for the analysis of oscillatory systems, essentially two general approaches are feasible:

(i) An approximate analytical one, based on the *harmonic balance method* approach;
(ii) A simulation one, employing contemporary simulation software, making use of conditioned switching between the solutions on a time-scale that is short in comparison to the dominant period of the excitation signal. The simulation approach enables use to be made of either the signum function approach, described by Eqs. (6) and (7) or a more physically sophisticated approach using the limit force analysis of Eqs. (8) and (6) and possibly also Eq. (10). The merits of both approaches have to be thoroughly assessed in the context of the specific case to be analysed.

One of the first rigorous approaches to computer simulation of the influence of friction in dynamic systems was undertaken by Karnopp [29]. He considers the causality issues and introduces a region of small relative velocity Dv_r around zero, indicated by the line segment in Fig. 2. Outside of this region the Coulomb approach is valid, whereas within this region F_f is determined by other forces acting in the system in such a way that the F_f remains within the region, until a breakaway force (i.e. the static friction force) is exceeded. He illustrates the advantages of this approach on various examples, using the bond graph approach for designing a set of appropriate conditions. The same methodology is essentially used in other applications, especially in rotary drives [4] or in dry friction dampers for turbo-machinery [5]; however, neither is related to the case analysed here.

3.2. The harmonic balance method

The harmonic balance method assumes a harmonic excitation by acceleration $\ddot{u}$ (with root mean square (rms) value a_{0u}) or rather by absolute displacement u with amplitude u_0 and variable angular frequency ω_x. The method is fully explained in standard textbooks—e.g. Refs. [6,13,14,30]. The equivalent damping around resonance b_e of a linear oscillator is introduced, depending on the amplitude of equivalent relative displacement ζ_e:

$$b_e = \frac{4F_{fk}}{\pi\zeta_e\omega_x}. \tag{11}$$

If the assumed harmonic solution is resolved then in steady state:

$$\zeta_e(\omega_x) = \frac{F_0}{k_x}\frac{\sqrt{1-\left(\frac{4F_{fk}}{\pi F_0}\right)^2}}{1-\left(\frac{\omega_x}{\omega_0}\right)^2}, \tag{12a}$$

where $F_0 = -mu_0\omega_x^2 = -\sqrt{2}ma_{0u}$ is the amplitude of an equivalent excitation force (in fact mass m inertial force amplitude in the stick state) and $\omega_0 = \sqrt{k_x/m}$ is the system natural frequency.

The formula can be expressed in a more transparent way:

$$\left|\frac{x_{ra}(\omega_x)}{\sqrt{2}a_{0u}/\omega_0^2}\right| = \left|1-\left(\frac{\omega_x}{\omega_0}\right)^2\right|^{-1}\sqrt{1-K^2} \tag{12b}$$

with a non-dimensional factor K after [31]:

$$K = \frac{4}{\pi}\frac{F_{fk}}{F_0}. \tag{12c}$$

The factor K will subsequently be termed the Den Hartog's factor and, except for a multiplicative constant, it relates the kinetic friction force F_{fk} to the equivalent excitation force F_0. Specifically for the horizontal oscillatory system of Fig. 1b with a constant normal force $F_N = mg_N$ the Den Hartog's factor K has the form (g_N is the gravity acceleration) [30]:

$$K = \frac{4}{\pi}\frac{\mu_k g_N}{\sqrt{2}a_{0u}}. \tag{12d}$$

Eq. (12b) describes the modulus of the frequency response function (FRF) of the relative displacement for harmonic excitation with constant displacement amplitude in the vicinity of the resonance. However, expressions (12a) and (12b) are approximate and valid only for $K<1$, i.e. for $F_0>(4/\pi)F_{fk}\cong 1.273F_{fk}$, i.e. for the base horizontal acceleration $a_{0u}>(2\sqrt{2}/\pi)g_N\mu_k$. In other words, the equivalent excitation force has to be sufficiently large in comparison to the kinetic friction force to permit the use of Eq. (12b).

For $F_0<F_{fk}$, or rather for $F_0<F_{fs}$, no movement is possible as the equivalent excitation force would not overcome the adhesion force. If $F_0\in(F_{fk},(4/\pi)F_{fk})\approx(F_{fk},1.273F_{fk})$ the movement is not purely harmonic, but has one or more stops within one period [2,6,13,31] and *is not described* by the above approximate formula, as $K\geqslant 1$ and the term under the square root is not real. If the frequency of excitation ω_x approaches ω_0, the amplitude of the oscillations at resonance will eventually grow beyond any limits [13,14]. The system behaves as an undamped one; however, with linearly increasing relative displacement amplitude x_{ra} of the oscillations [14,30] until the structural limit at x_{rM} would be reached.

The case with both the viscous and the dry friction damping of Fig. 3a can be solved too, using the harmonic balance method [2] however the formulas are somehow cumbersome. Other usage of the harmonic balance method is illustrated for example in Ref. [32].

The Den Hartog's approach cannot account for the stick–slip phenomenon, which is accounted for by a procedure illustrated in Refs. [7,9] for therein described specific cases under harmonic excitation. None is applicable when random excitation is assumed, as often occurs in practice. This is especially so, if the equivalent excitation force amplitude $F_0 = \sqrt{2}ma_{0u}$ would randomly fluctuate below F_{fk} and above $(4/\pi)F_{fk}$

and the relative velocity v_r would be low, i.e. if the friction force would be commeasurable with the equivalent excitation force of the isolated body.

3.3. Use of the signum function

Use of the signum function for the simulation of an oscillatory system as in Fig. 3d is an easy option that is facilitated by any simulation software. The equation describing the motion has the form (4), repeated here as follows:

$$\text{for } v_r \neq 0: \quad m\ddot{x}_r + k_x x_r + b\dot{x}_r + F_f \operatorname{sgn}(\dot{x}_r) = -m\ddot{u}. \tag{13}$$

For $v_r = 0$ the sgn function is set to zero [3,6,26,33] and thus *analysis for $v_r = 0$ is completely omitted.* Sometimes the discontinuous signum function (7) is substituted by a "smoothed" continuous function, which approximates the sgn function with a required degree of accuracy [20,25]:

$$\operatorname{sgn}(v_r) \approx \frac{2}{\pi}\arctan(cv_r) \approx \tanh(cv_r) \approx \operatorname{erf}(cv_r) \approx \frac{cv_r}{1 + c|v_r|}. \tag{14}$$

Constant c in each of the functions describes the numerical "match" between the sgn function and the respective continuous function used for the approximation. The selection should be governed by the following rules [20]:

- if it were too small the approximation would differ excessively from the sought non-smooth one;
- if it were too large the computation effort is too great and the approximation is not sufficiently smooth.

In Ref. [25] selected numerical values are analysed. It is demonstrated, that a value of $c \geqslant 10^3$ suffices to fulfil both conditions and the fit with the analytical solution is within 1%. It is suggested that the last formula is better with regards to the computational speed in attaining the same level of accuracy. In a more recent paper of the same author [34] the tanh approximation is advocated, as this is an exact representation of the sgn function in the sense of the so-called non-standard analysis.

Any of the above-mentioned approaches circumvents the problem of solving differential equation (13) with the discontinuous non-smooth signum function by introducing a continuous smooth function with an arbitrary large derivative at zero crossing.

3.4. Use of the stick–slip approach

If the stick–slip phenomena are to be accounted for, as indicated by Eq. (8)—case of Fig. 3b, following approach has to be followed:

1. For $v_r \neq 0$ Eq. (13) is valid;
2. When the $v_r \neq 0$ to $v_r = 0$ transient occurs, the relative movement stops and the force balance condition across the friction interface has to be tested by the following set of conditions:

$$\text{(i) Slipping}: \ |v_r| > \varepsilon \text{ or } |F_L| < F_{fs}, \tag{15a}$$

$$\text{(ii) Sticking}: \ |v_r| < \varepsilon \text{ and } |F_L| < F_{fs}, \tag{15b}$$

$$\text{while}: \ F_L = m\ddot{x} + k_x x_r \tag{16}$$

and ε is a sufficiently small number, representing numerically the close vicinity of zero.

Conditions (15) can be expanded further into a more subtle set of conditions, assuming that the oscillatory system is already in motion:

(a) $|v_r| > \varepsilon$, i.e. Eq. (13) holds and no state change occurs.

(b) $|v_r| \leqslant \varepsilon$ and concurrently $|F_L| > F_{fk}$. The oscillatory system passes the $|v_r| \leqslant \varepsilon$ margin and continues its movement without stopping. Eq. (13) holds and no state change occurs.

(c) $|v_r| \leqslant \varepsilon$ and concurrently $|F_L| < F_{fk}$. The oscillatory systems stops abruptly and state change occurs. The adhesive forces take over the control of the friction. The system is in a relative standstill at $v_r = 0$ and from this time instant on the condition $|F_L| \geqslant F_{fs}$ has to be tested in a loop.
(d) As soon as the condition $|F_L| \geqslant F_{fs}$ is met the system starts to move abruptly again. A state change occurs, $|v_r|$ becomes $> \varepsilon$ and the kinetic friction forces take over. Eq. (13) has to be re-solved with the actual initial conditions resulting from case (c).
(e) Then the testing of condition $|v_r| > \varepsilon$ is to be repeated.
(f) If the oscillatory system starts from rest, the condition $|F_L| \geqslant F_{fs}$ has to be met first, before any relative movement is possible.

3. The fulfilment of the constraint $x_{ra} < x_{rM}$ has to be tested too.
4. For the $v_r = 0$ to $|v_r| \neq 0$ transient, the Gaussian approximation (10) for smoothing the transient may be used.

This approach follows that one of Karnopp [29], using $\varepsilon \sim D v_r$; however, the bond theory is not applied. Instead, the operation for the numerical evaluation of the condition $v_r = 0$ is analysed in more detail.

3.5. The determination of the condition $v_r = 0$

The operation of determining when v_r reaches zero, or in numerical systems rather the condition $|v_r| < \varepsilon$, is generally called "variable zero-crossing operation" and is facilitated in the standard simulation software by specific procedures (see e.g. Ref. [33]). The main difficulty for numerical systems with equal time increments is the need for a precise determination of the time instant, when the zero-crossing occurs, or when $|v_r| < \varepsilon$, while the value of ε has to be assessed independently. This is very important when processing the real-world data (as occurring in the ground transportation, for example), commonly sampled at equal time increments. *The standard stiff ordinary differential* equations *solvers with variable time increment are not applicable*, unless the sampled data set would be re-interpolated in the same way. Another approach is to develop an ordinary differential equations solver with a fixed time increment, which specifically caters for determining the $|v_r| < \varepsilon$ condition within the given fixed time increment Δt, as was the case here. In general two methods are feasible:

(i) The close to zero neighbourhood identification method is based on the assumption that the value of v_r is set to zero if $|v_r| < \varepsilon$. This simple method is limited by the sensitivity to the proper estimation of the variable ε. However, for the random excitation no forward prediction of the v_r is feasible, so it is very difficult to state optimal ε beforehand.
(ii) The backward zero-crossing detection method is a common feature of the iterative numerical solutions of algebraic equations. Detection is done by evaluation of the product of the relative velocities in two adjacent steps at t_{i-1} and t_i:
   (a) if $v_{r(i-1)} v_{r(i)} < 0$-zero-crossing occurred;
   (b) if $v_{r(i-1)} v_{r(i)} > 0$-zero-crossing did not occur.

In the case of positive detection of zero-crossing, the point at t_i is rejected and a more precise determination of the zero-crossing point is further performed using bisection, interpolation or step-size reduction. Both methods have to be combined.

The step size Δt is crucial for proper simulation of a stiff system of ordinary differential equations in numerical simulation systems [3,4,25]. In the context of the system analysed here, a fixed equidistant time step Δt was used. Increase of Δt is advantageous for reducing the duration of the simulation process (reducing mainly the processing time). On the other hand Δt that is too small can rapidly increase numerical error and the rate of its propagation. Therefore, optimisation of the simulation parameters should always precede simulation itself [3,4]. The use of a robust Runge–Kutta integration method of the fourth-order yields, in authors' experience, acceptable results. An optimal value for Δt can be determined either analytically or by trial-and-error method. However, the step size must be always chosen in such a way, that within time interval of $2\Delta t$, the excitation signal does not return below the sticking limit. If this happens, false numerical oscillations, which have no relation to the physical processes at the contact interface, occur, as illustrated

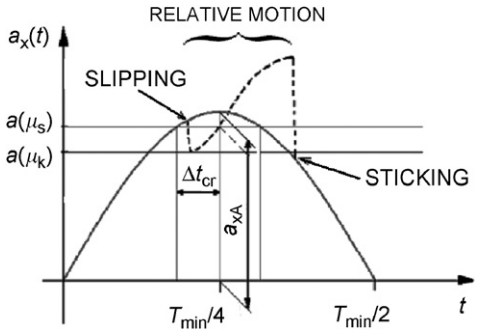

Fig. 4. Explanation of the step size Δt.

below. Analytical determination of Δt requires evaluation of the following excitation parameters, assuming harmonic excitation (see Fig. 4):

(a) Maximum excitation frequency $f_{\max} = 1/T_{\min}$ that should be covered by the simulation, emerging from analysis of the particular problem. For non-harmonic excitation estimation of an equivalent maximal frequency is needed, assessed for the particular problem to be analysed.
(b) Estimation of the relative overlap q by which the excitation acceleration amplitude a_{xA} at $T_{\min}/4$ exceeds the limit acceleration $a(\mu_s)$ corresponding to the static friction F_{fs}. This parameter represents the tolerance to neglected starts in the time history of the simulation, i.e. the tolerance to neglected possible stick $\Rightarrow$ slip transitions. The value of q depends on the accuracy of μ_s value and should be within 1.001 and 1.100. The amplitude of the assumed excitation acceleration limit is then $a_{xA} = qa(\mu_s)$. Then the critical maximum step size $\Delta t_{\rm cr}$ is given by the formula (see also Fig. 4):

$$\Delta t \leqslant \Delta t_{\rm cr} = \frac{[\pi/2 - \arcsin(1/q)]}{2\pi f_{\max}} = \frac{[\pi/2 - \arcsin(1/q)]}{\omega_{\max}}. \tag{17}$$

4. Detailed illustration of the dry friction force simulation approaches

4.1. Introduction

In the following section, an example of the application of both simulation approaches—the signum approach and the stick–slip approach will be illustrated. But first an important matter has to be noted—due to the system nonlinearity it has to be decided in advance which system transmissibility characteristics are to be analysed—either the absolute displacement transmissibility characteristics or the absolute acceleration transmissibility characteristics. In a linear sdof oscillatory system there is a straightforward relation between these characteristics, however this is not so for nonlinear systems. As already noted above in respect to Ref. [11], great care must be taken when inferring from results obtained for the displacement transmissibility on the behaviour described by the acceleration transmissibility characteristics.

The translational accelerations are most often the measured variables in ground transportation. Hence, in the following deliberations the acceleration transmissibility characteristics will be analysed, augmented by the relative displacement transmissibility characteristics. The latter will be used just for testing the condition $x_{ra} < x_{rM}$ to limit the relative displacement (stroke) in relation to the structural constraints, especially around the natural frequency. This can be an important issue in the ground vehicles and their suspension systems or suspended driver's seats.

The example is based on a sdof oscillatory system with both dry friction and viscous energy dissipation, as depicted on Fig. 1b, equation of motion of which was given above as Eq. (13). Let the mass $m = 75\,\text{kg}$, spring stiffness $k_x = 7500\,\text{N m}^{-1}$, giving an undamped natural angular frequency $\omega_0 = 10.0\,\text{rad s}^{-1}$, i.e. system natural frequency of $f_0 = 1.592\,\text{Hz}$. Let us assume a linear damping coefficient of value of $b = 500\,\text{N s m}^{-1}$

(i.e. damping ratio $\xi = 0.333$ and damped natural frequency $f_d = 1.50\,\mathrm{Hz}$). The maximum relative displacement amplitude x_{rM} is limited to $\pm 25\,\mathrm{mm}$. This is a good generic example of a horizontal suspension system of a contemporary driver's seat. Two cases will be analysed, further on denoted as "low dry friction" and "high dry friction" cases, both essentially corresponding to the case depicted in Fig. 3a:

(i) The low dry friction case of $F_{fk} = 15\,\mathrm{N}$.

(ii) The high dry friction case of $F_{fk} = 45\,\mathrm{N}$.

These values were chosen, based on the experience, to be representative of driver' seats [35].

Due to the inherent nonlinearity the standard approach of calculating the frequency response function for the assumed harmonic excitation with constant acceleration amplitude is not viable. Instead, the ratio of response $\ddot{x}$ rms value a_{0x} to the excitation $\ddot{u}$ rms value a_{0u} is calculated. This corresponds to the acceleration transmissibility magnitude for the given excitation signal. Here such ratios are calculated for constant excitation acceleration rms values $a_{0u} = 0.50,\ 0.75$ and $1.0\,\mathrm{m\,s^{-2}}$. A harmonic excitation is used with frequency step of 0.1 Hz in the frequency band 0.5–10.0 Hz. By the same approach the relative displacement characteristic x_{0r}/u_0, corresponding to the ratio of relative displacement x_r rms value x_{0r} to base displacement u rms value u_0, is calculated and its maximum is checked against x_{rM}, while $u_0 = \sqrt{2}a_{0u}/\omega_x^2$, where ω_x is the excitation angular frequency.

4.2. Illustration of the signum approach

The results of the simulation programme employing the signum function approximation by the last formula of Eq. (14) with constant $c = 1 \times 10^4$ and fixed integration step $\Delta t = 0.01\,\mathrm{s}$, are graphically depicted in Fig. 5 for the low dry friction case and in Fig. 6 for the high dry friction case. For reference, the response curve of a viscously damped sdof oscillator without dry friction (cf. Fig. 3c) is shown, too. This one is subjected to the same excitation, which gives a relative displacement at the damped natural frequency f_d of 23 mm, i.e. just below the set maximum of $x_{rM} = 25\,\mathrm{mm}$.

The graphs for the high dry friction force value in Fig. 6 provide a good illustration from which to interpret the influence of the friction. First, there is a clear difference to the frictionless sdof response at the frequencies above $\sqrt{2}f_0 \approx 2.25\,\mathrm{Hz}$. The dependence of the acceleration transmissibility on the excitation amplitude is much greater than for the sdof approach with the low dry friction force (Fig. 5). For low excitation amplitude, $a_{0u} \approx 0.50\,\mathrm{m\,s^{-2}}$, the acceleration transmissibility value hovers around unity. This indicates that the oscillatory system is at a standstill and no attenuation of vibration occurs, while Den Hartog's factor $K \cong 1.08 > 1$. Also, the relative displacement transmissibility does not reach unity value at higher frequencies, but for $a_{0u} \approx 0.50\,\mathrm{m\,s^{-2}}$ hovers

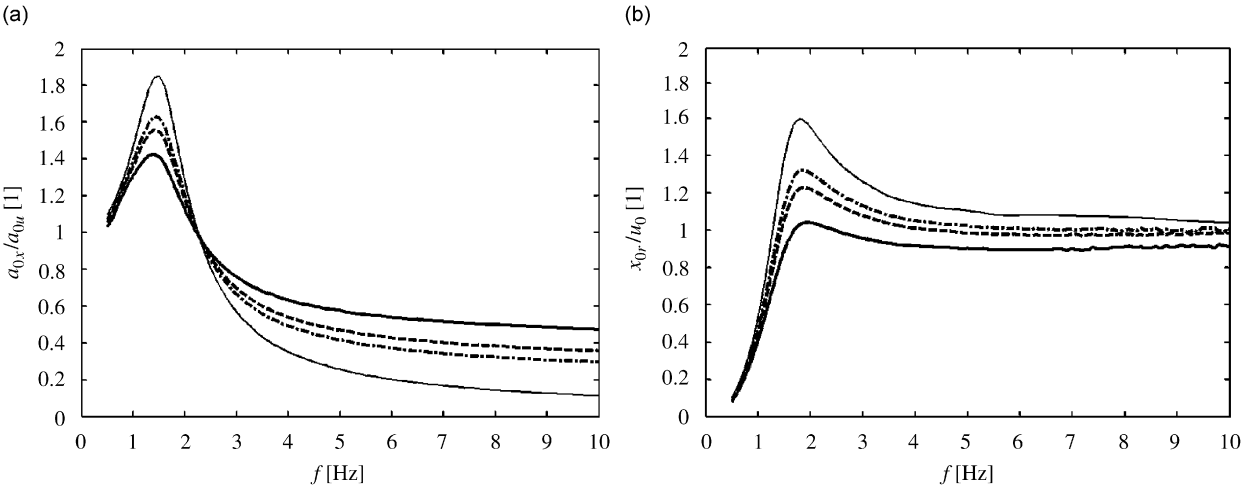

Fig. 5. Curves of (a) acceleration transmissibility and (b) relative displacement transmissibility for sdof oscillatory system with low dry friction force $F_{fk} = 15\,\mathrm{N}$ for three excitation intensities $a_{0u} = 0.50\,\mathrm{m\,s^{-2}}$ (——), $0.75\,\mathrm{m\,s^{-2}}$ (— —), $1.00\,\mathrm{m\,s^{-2}}$ (— • —) and reference $F_{fk} = 0\,\mathrm{N}$ (——), predicted using the signum function.

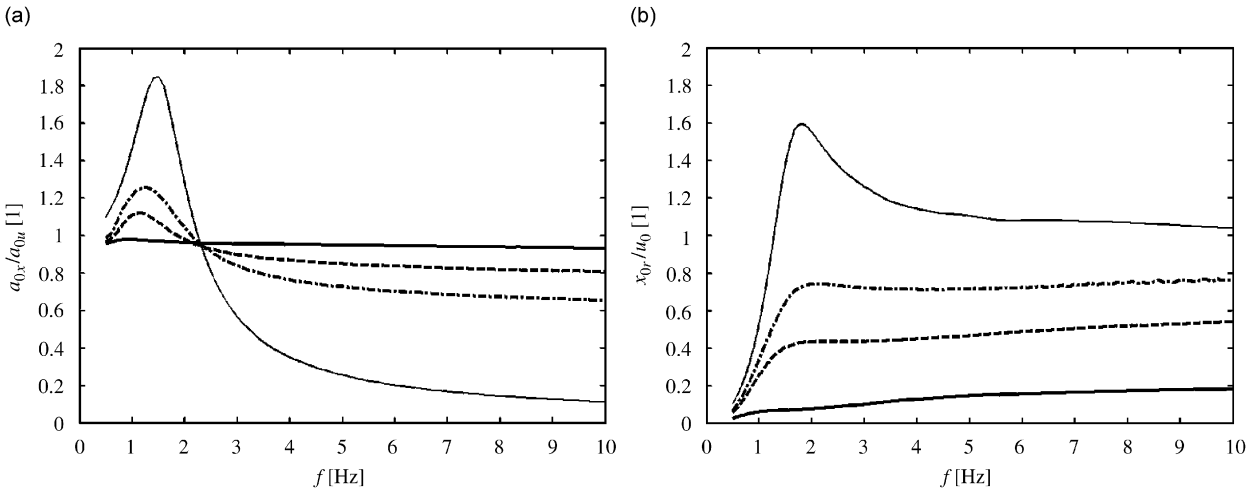

Fig. 6. Curves of (a) acceleration transmissibility and (b) relative displacement transmissibility for sdof oscillatory system with high dry friction force $F_{fk} = 45\,\mathrm{N}$ for three excitation intensities $a_{0u} = 0.50\,\mathrm{m\,s^{-2}}$ (——), $0.75\,\mathrm{m\,s^{-2}}$ (— —), $1.00\,\mathrm{m\,s^{-2}}$ (— • —) and reference $F_{fk} = 0\,\mathrm{N}$ (——), predicted using the signum function.

around zero, again indicating system standstill. For the larger acceleration intensities the vibration attenuation above $\sqrt{2}f_0$ is smaller than would by expected from the analysis of a frictionless sdof oscillatory system.

The acceleration amplification around the damped natural frequency f_d, due to the influence of friction decreases, as expected, which is best seen for the lower dry friction force value (Fig. 5). The decrease of the amplification (increase in the damping) at f_d is dependant on the excitation amplitude and is more pronounced for the system with the higher dry friction value, $F_{fk} = 45\,\mathrm{N}$. Hence a sdof oscillatory system with dry friction has better vibration attenuation properties around f_d than the sdof system without friction. Also the relative displacement transmissibility is smaller than that for the frictionless sdof oscillatory system; hence the constraint $x_r < x_{rM}$ is fulfilled.

The influence of the dry friction force on the vibration attenuation properties of the nonlinear system can be further illustrated by the acceleration transmissibility curve (in log–log representation) for steady-state acceleration for value $a_{0u} = 0.75\,\mathrm{m\,s^{-2}}$ (Fig. 7) (with $K \cong 0.72 < 1$). Note that even the low dry friction force value severely decreases the vibration attenuation of the system at frequencies above $\sqrt{2}f_0$. Moreover, the figure illustrates the possible margin of vibration attenuation (hatched), which would enable the vibration attenuation to be improved by reducing the dry friction force. However, no complete removal of the dry friction is in reality possible, hence a real system would always have worse vibration attenuation properties above $\sqrt{2}f_0$ than the frictionless sdof system analysis would indicate.

It is interesting to note the frequency dependence of the maximum of respective dissipative components—viscous damper force $F_{vd} = bv_r$ and friction force $|F_f|$, depicted in Fig. 8. Note, that the friction component is independent of the excitation frequency, whereas the viscous component F_{vd} is not:

- For the low friction value $F_{fk} = 15\,\mathrm{N}$ (Fig. 8a) the viscous damping term is larger around f_d than the constant friction force F_{fk}. There is an intermittent frequency range, where both terms have approximately the same magnitude, while with increasing excitation frequency the dry friction term takes over the vibratory energy dissipation.
- For the high friction value $F_{fk} = 45\,\mathrm{N}$ (Fig. 8b) the constant friction term dominates the whole frequency range. The viscous damping is pronounced most at f_d; however, making only 66% of the former.

4.3. The stick–slip approach

The same parameters were used in a more sophisticated simulation programme, accounting for the stick–slip phenomena, according to Eqs. (15a,b) and (16). The simulation results are shown in Fig. 9 for

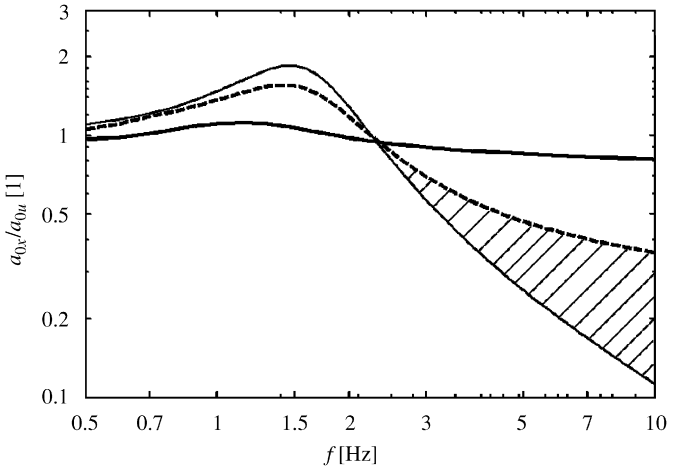

Fig. 7. Illustration of the dry friction force influence for $a_{0u} = 0.75\,\mathrm{m\,s^{-2}}$ on vibration mitigation properties: $F_{fk} = 0\,\mathrm{N}$ (——), $F_{fk} = 15\,\mathrm{N}$ (— —), $F_{fk} = 45\,\mathrm{N}$ (——).

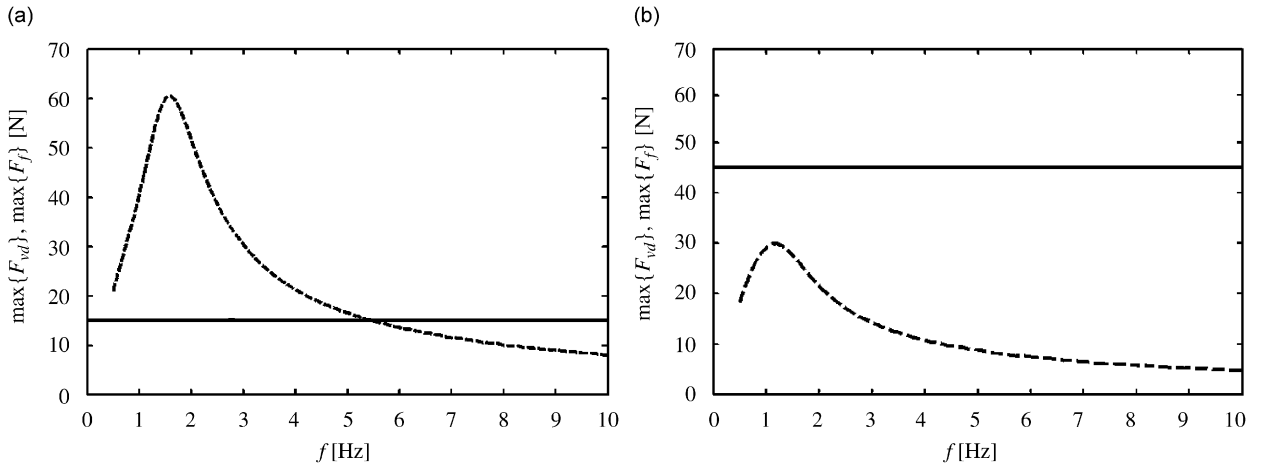

Fig. 8. Illustration of the dry friction force influence for $a_{0u} = 0.75\,\mathrm{m\,s^{-2}}$ on the relation between maximum values of the two dissipative components F_{vd} (— —) and F_f (——), respectively: (a) $F_{fk} = 15\,\mathrm{N}$ and (b) $F_{fk} = 45\,\mathrm{N}$.

$F_{fk} = 15\,\mathrm{N}$ and in Fig. 10 for $F_{fk} = 45\,\mathrm{N}$. The respective adhesive friction force F_{fs} was in both cases assumed to be larger than F_{fk} by 20%. For reference, the response curve for a viscously damped sdof frictionless oscillator is shown for the same excitation. The maximum of the limiting force (Eq. (16)) for $a_{0u} = 0.50\,\mathrm{m\,s^{-2}}$ and $x_r = 0\,\mathrm{mm}$ is 53 N, while $F_{fs} = 54\,\mathrm{N}$, i.e. the oscillatory system is in permanent sticking state with $K \cong 1.08 > 1$, as already noted above. This is clearly seen in Fig. 10b (the bold line); however, not in Fig. 6b (the bold line) obtained for the signum approach. Hence, the signum approach in the case of permanent sticking (locked system) provides a result which is not correct. Note that in this state no energy dissipation is possible. The oscillatory system moves as a rigid body.

The stick–slip model enables calculation of the ratio ρ defined as the time when the oscillatory system is in the stick state as a percentage of the total duration of the simulation. The respective values of ρ for the two dry friction force values, as a function of frequency, are depicted in Fig. 11, omitting the obvious value of $\rho = 100\%$ for the permanent sticking state for $a_{0u} = 0.50\,\mathrm{m\,s^{-2}}$.

It is seen from Fig. 11 that in the frequency band below system natural frequency f_0 there is always a region, where the system remains in a standstill for a while (twice during the oscillation period), as already noted.

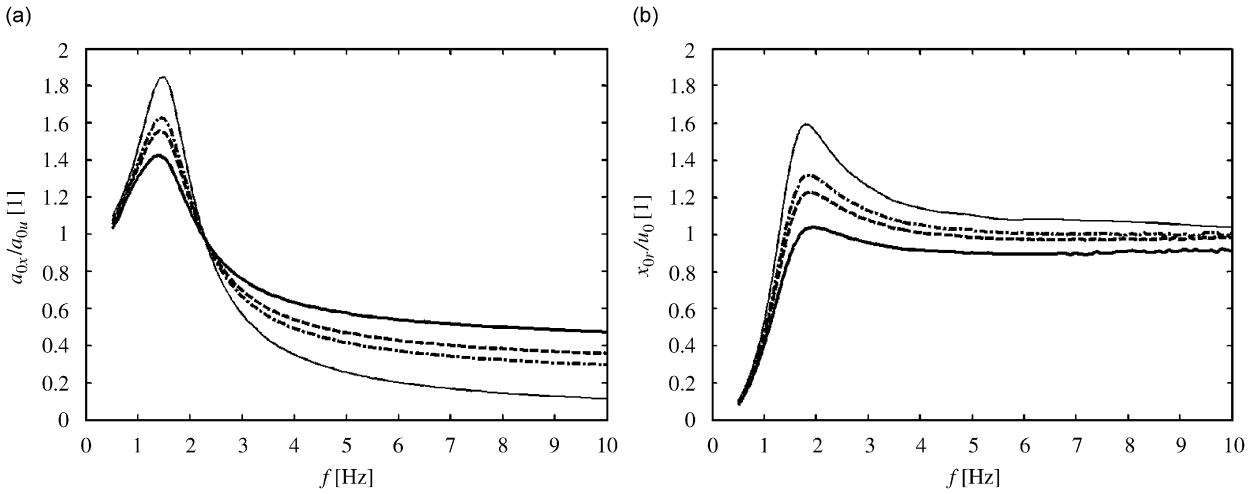

Fig. 9. Transfer function estimates for sdof oscillatory system with low dry friction force $F_{fk} = 15\,\mathrm{N}$ for three excitation intensities $a_{0u} = 0.50\,\mathrm{m\,s^{-2}}$ (——), $0.75\,\mathrm{m\,s^{-2}}$ (— —), $1.00\,\mathrm{m\,s^{-2}}$ (— • —) and reference $F_{fk} = 0\,\mathrm{N}$ (——), predicted using the stick–slip approach.

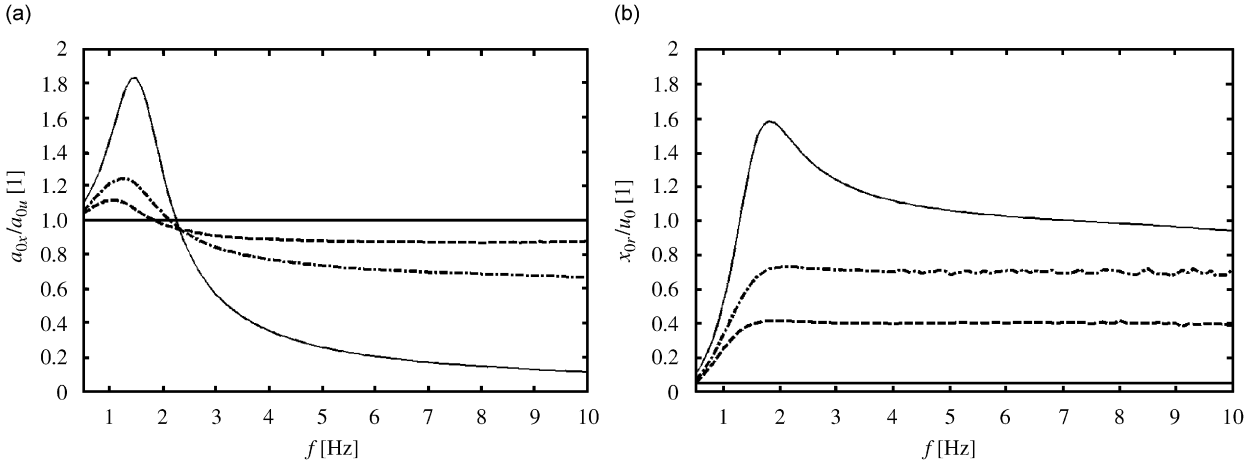

Fig. 10. Transfer function estimates for sdof oscillatory system with high dry friction force $F_{fk} = 45\,\mathrm{N}$ for three excitation intensities $a_{0u} = 0.50\,\mathrm{m\,s^{-2}}$ (——), $0.75\,\mathrm{m\,s^{-2}}$ (— —), $1.00\,\mathrm{m\,s^{-2}}$ (— • —) and reference $F_{fk} = 0\,\mathrm{N}$ (——), predicted using the stick–slip approach.

For the high friction case $F_{fk} = 45\,\mathrm{N}$ there are two limit cases: For the acceleration $a_{0u} = 1.00\,\mathrm{m\,s^{-2}}$ there is no stopping due to the friction, because the equivalent excitation force exceeds the F_{fk} value at $v_r = 0$ and the mass moves continuously through the ε boundary. For $a_{0u} = 0.50\,\mathrm{m\,s^{-2}}$ the system is in permanent sticking state. For excitation acceleration $a_{0u} = 0.75\,\mathrm{m\,s^{-2}}$ the oscillatory system is in a stick state approximately 16.3% of the total simulation time.

It might be interesting to inspect the time history of the response signals in more detail. Fig. 12 shows the relative displacement x_r; the relative velocity $v_r \equiv \dot{x}_r$; absolute acceleration $a_x = \ddot{x}$ of the oscillating mass m for two excitation frequencies: $0.5 \times f_0$ and $2 \times f_0$ while the corresponding frictionless sdof natural frequency is $f_0 = 1.592\,\mathrm{Hz}$, simulation step size $\Delta t = 0.001\,\mathrm{s}$.

From these time courses for harmonic excitation the following observations can be made:

(i) For the sub-resonance domain two stops in each period are visible in the relative velocity v_r courses whereas for the domain above resonance this occurs only for the higher friction case.

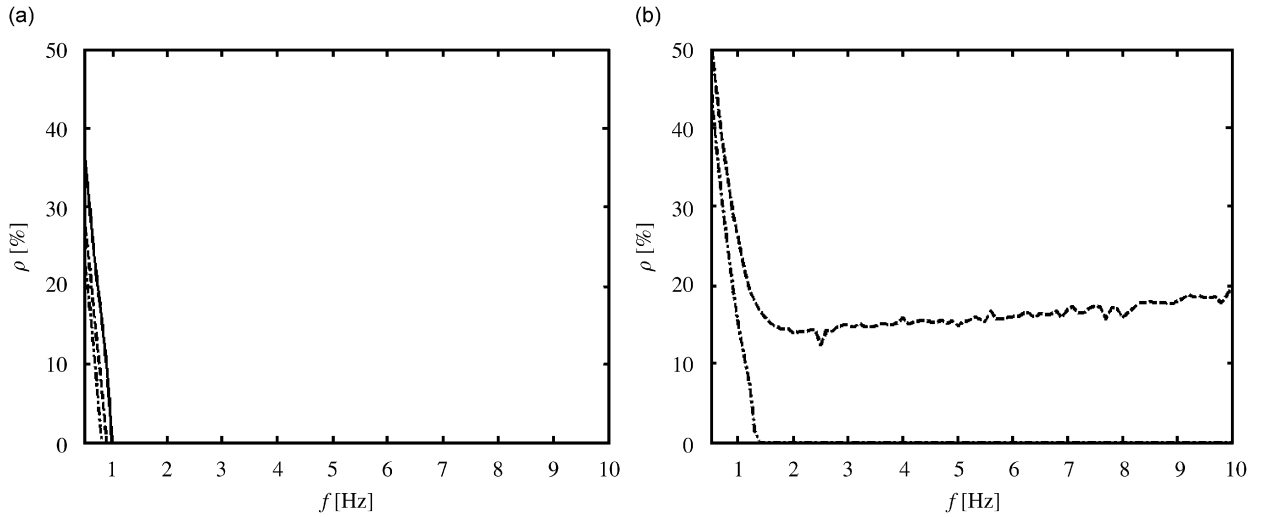

Fig. 11. Frequency dependence of ratio ρ for different excitation intensities $a_{0u} = 0.50\,\mathrm{m\,s^{-2}}$ (——), $0.75\,\mathrm{m\,s^{-2}}$ (— —), $1.00\,\mathrm{m\,s^{-2}}$ (— • —): (a) $F_{fk} = 15\,\mathrm{N}$ and (b) $F_{fk} = 45\,\mathrm{N}$.

(ii) These stops are visible also in the x_r courses and in the response accelerations as the sections where the response follows the input, preceded by short "hitches" due to the change in friction state (kinetic to adhesive). There is not much difference between the acceleration courses for both dry friction values.

(iii) For the region above the resonance and the low friction case the oscillatory system overshoots the $v_r = 0$ state without stopping, hence no changes in x_r and v_r are noticeable. However a shift of the order of $2F_{fk}/m \approx 0.40\,\mathrm{m\,s^{-2}}$ can be observed in the acceleration time course. This is due to reversing the dry friction force direction at $v_r = 0$.

(iv) For the region above resonance with the high friction, two stops in one period are observable in the v_r course, but are not noticeable in x_r course.

(v) For the region above resonance with the high friction, the vibration dissipation by the dry friction force is prevailing (see Fig. 8b), hence the acceleration course resembles a rectangular wave with a large content of higher harmonics rather than a sinusoid. However, a short stop is visible at a point where the acceleration follows the excitation, as well as the "hitch" due to the change in the friction state (kinetic to adhesive). If $F_{fs} = F_{fk}$ the "hitch" would not be present.

It can be concluded that the time courses correspond well to the state switching conditions hence the simulation works as expected. Moreover the response acceleration courses indicate a component with rectangular time course with large content of higher harmonics, causing harshness in the response, even for the low-friction case.

Next, the influence of the integration period Δt can be illustrated on a numerical example with harmonic excitation. As already noted the sampling frequency of field measured signals is set independently of the simulation requirements and cannot be usually changed. Hence the simulation integration period has to follow the sampling period, if comparison of simulation results to real measured signals is sought. Let us assume harmonic excitation of the system described above at a frequency $0.5 \times f_0 \approx 0.796\,\mathrm{Hz}$ and with $a_{0u} = 0.55\,\mathrm{m\,s^{-2}}$, i.e. slightly above the stick limit ($K \cong 0.98 < 1$). A simulation has been undertaken in turn with integration time steps $\Delta t = 0.01$ and $0.001\,\mathrm{s}$. The time curves of the response accelerations for both approaches are depicted in Fig. 13 for $F_{fk} = 45\,\mathrm{N}$ and for $F_{fk} = 15\,\mathrm{N}$. The parasitic oscillatory phenomenon is clearly present for $F_{fk} = 45\,\mathrm{N}$ if $\Delta t = 0.01\,\mathrm{s}$, corresponding to the real signal sampling frequency, however not for $\Delta t = 0.001\,\mathrm{s}$. This would be a proper simulation time step for the signum approach, if no comparison to measured signal were sought.

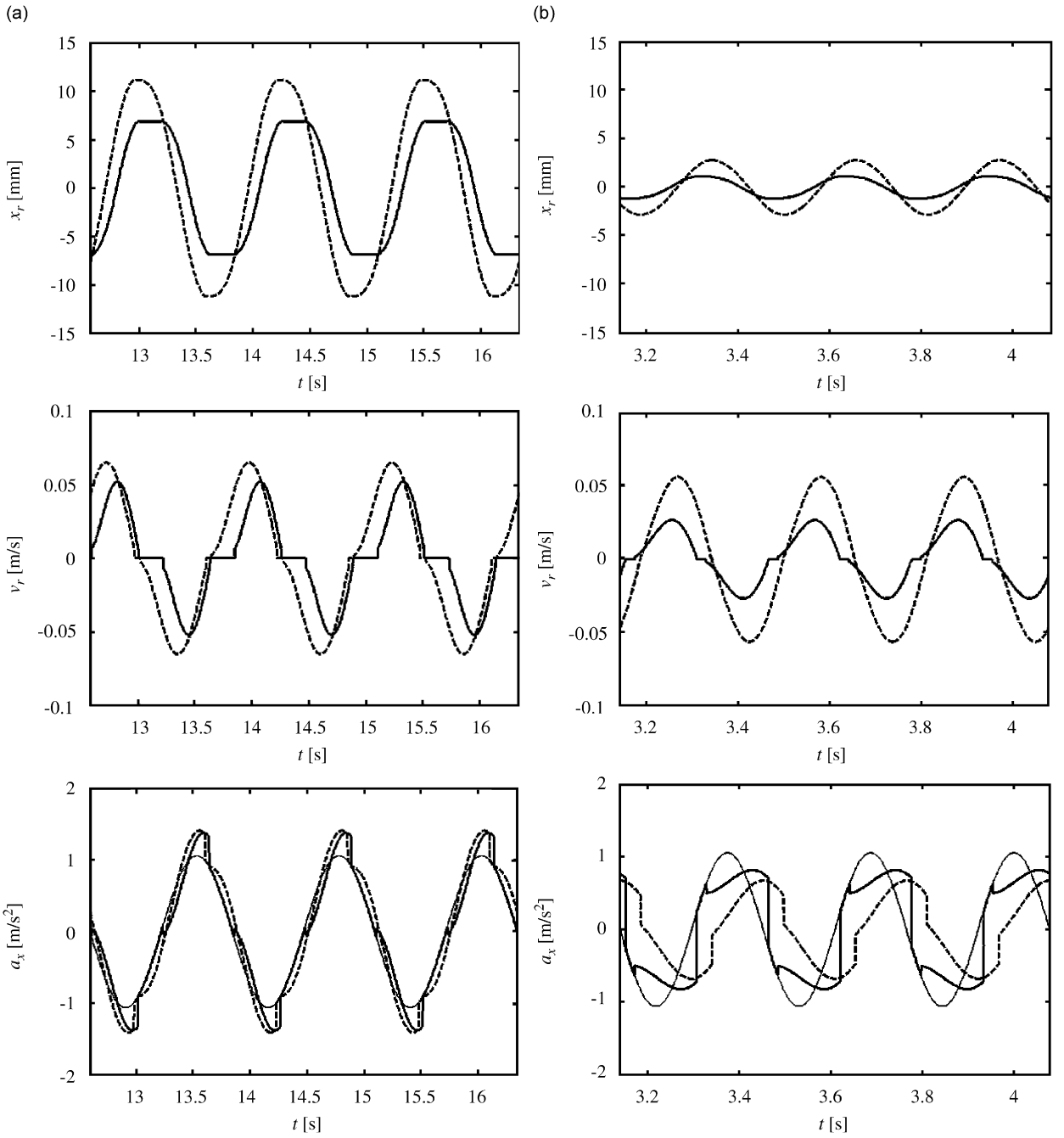

Fig. 12. Time histories of system variables for different excitation frequencies for $F_{fk} = 15\,\mathrm{N}$ (— —) and $F_{fk} = 45\,\mathrm{N}$ (——): (a) $0.5 \times f_0$, (b) $2 \times f_0$, predicted using the stick–slip approach.

5. Comparison of the two dry friction force simulation approaches

In the previous section, the performance of the two approaches to analyse steady-state harmonic excitation was thoroughly reviewed and some small advantages of the second approach were demonstrated. In this section, the differences are highlighted in a different way.

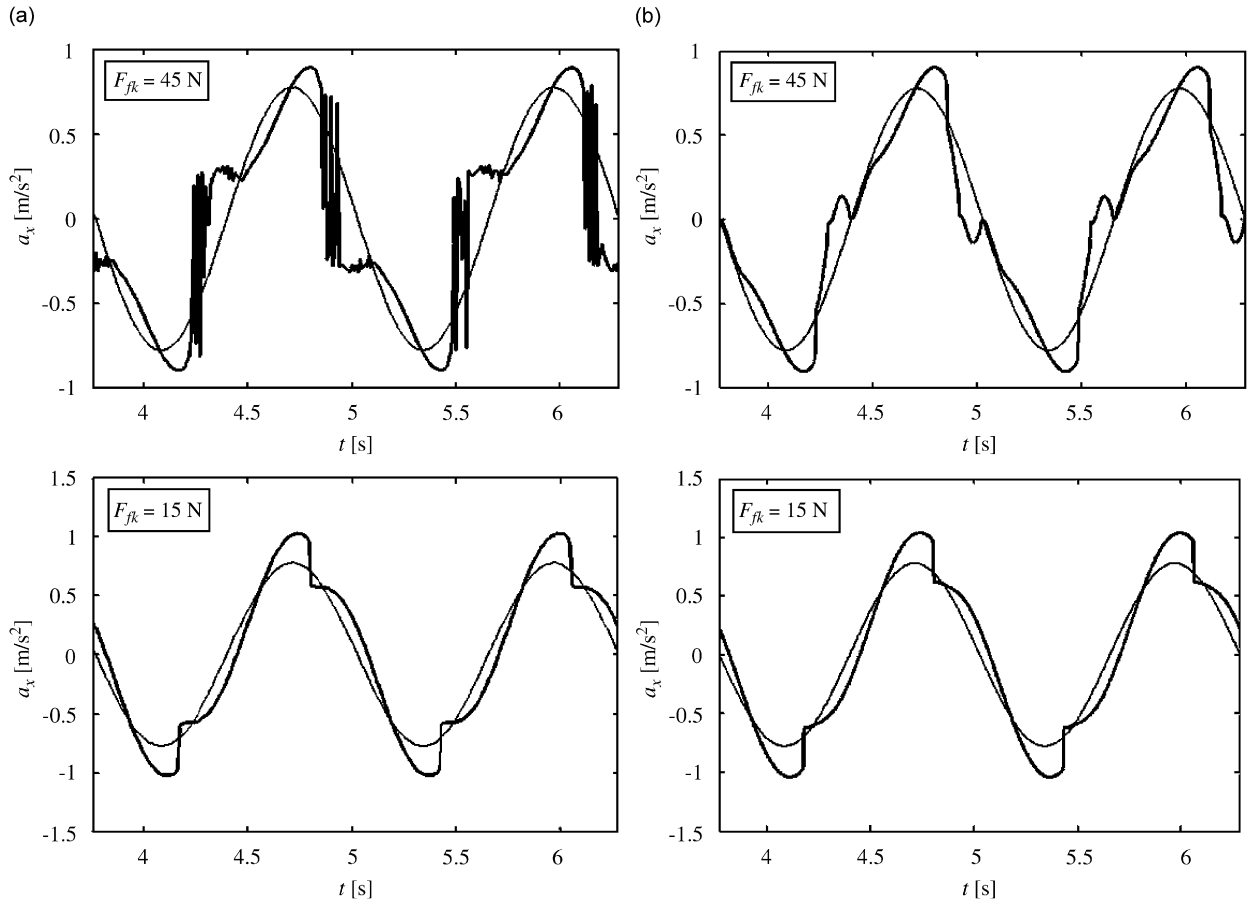

Fig. 13. Time histories of the acceleration responses of an sdof oscillatory system with friction force under harmonic excitation in respect to different integration steps: (a) $\Delta t = 0.01$ s and (b) $\Delta t = 0.001$ s.

In many applications time courses of different variables are less important, while aggregate and statistical characteristics are preferred, e.g. maximum and minimum values, rms value, crest factors, power spectral density (PSD), amplitude distribution, etc. Here the acceleration rms values will be used, as explained above. Moreover, the dry friction value might be much higher than in the previous example, as actually observed [35].

When the signum function method is used, a high friction value in combination with a low v_r results in numerical instability. The numerical instability causes parasitic oscillations in the time interval where v_r course is crossing the zero value. The error appears in the response acceleration and not in the relative displacement. It can be explained in the following way: the sign output of the signum function for the ith step is determined by the value in the $(i-1)$th step. In the vicinity of the zero crossing point the signum function forces the value for the next step to have the opposite sign and vice versa. If the simulation interval Δt is too large, or the v_r change is too slow, false oscillations with period $2\Delta t$ occur, even if the real system would stop due to the friction. In simulation studies this can be circumvented by setting a sufficiently small Δt at the expenses of the simulation time. In analysing real world sampled data, the time interval is set at the time of data acquisition, and later comparison by simulation means has to follow suit, or the sampled data would have to be re-sampled. Thus, the choice of simulation interval Δt is limited to some extent. If the simulation interval is too large *parasitic oscillations occur when using the signum approach. However, these oscillations do not occur when using the physically correct stick–slip approach.* This will be illustrated in more detail below, based on the field measured data collected as follows:

Fore-and-aft accelerations were recorded on a driver's seat below and above the horizontal suspension system. The seat was mounted in the cabin of an articulated truck, loaded with 22 tones of ballast and driven

on a highway with a constant speed of 70 km. The accelerations were measured using a B&K 4368 accelerometer connected to a B&K 2635 conditioning amplifier and recorded on-board by a Sony 204A DAT recorder with sampling frequency of 12 kHz. The test signal time history, decimated at sampling frequency 100 Hz is shown in Fig. 14.

The difference between both approaches is illustrated firstly by Fig. 15. The same system as described above is subjected to random input acceleration excitation $a_{0u} = 0.35\,\mathrm{m\,s^{-2}}$, the time history of which is depicted in Fig. 14. Note false oscillations for $F_{fk} = 45\,\mathrm{N}$; a consequence of which is a markedly different acceleration rms value obtained by evaluating the output signal from the model using the stick–slip approach ($a_{0x} = 0.33\,\mathrm{m\,s^{-2}}$), compared with the signum approach, which gives $a_{0x} = 0.50\,\mathrm{m\,s^{-2}}$. The difference is not marked for the lower $F_{fk} = 15\,\mathrm{N}$ (0.20 versus 0.21 $\mathrm{m\,s^{-2}}$), where virtually no sticking occurs in the time interval shown. This example illustrates bluntly the principal drawback of the signum method applied to oscillatory systems in which the equivalent excitation force may fluctuate around the dry friction force.

Furthermore to Fig. 15 it is interesting to explore the influence of dry friction force magnitude on the system behaviour in more general way, using the aggregate performance description by respective rms values. In Fig. 16a, the curves that relate the ratios a_{0x}/a_{0u} to variable F_{fk} for two different random excitation intensities $a_{0u} = 0.35$ and $a_{0u} = 0.67\,\mathrm{m\,s^{-2}}$ are depicted. The selected random excitation time records were some of those actually measured in the field tests described above, one of them being that one illustrated in Fig. 14. Also the ratio a_{0x}/a_{0u} as a function of the variable F_{fk} for the lower intensity $a_{0u} = 0.35\,\mathrm{m\,s^{-2}}$ obtained using the signum approach is depicted by a thin line. Note the large discrepancy between this and the ratio

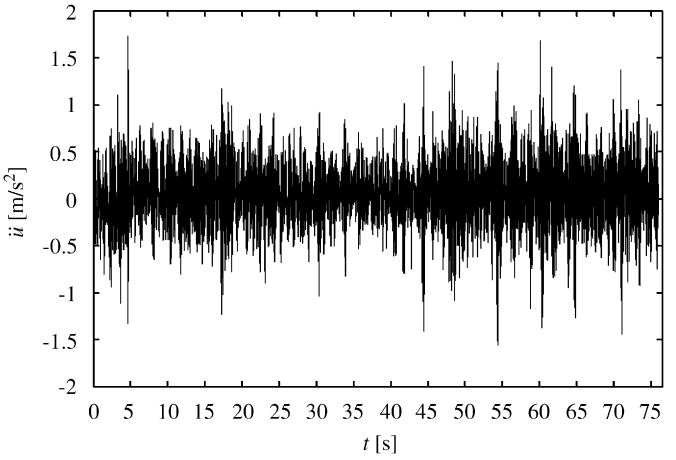

Fig. 14. Time history of the random excitation acceleration of the horizontal suspension system.

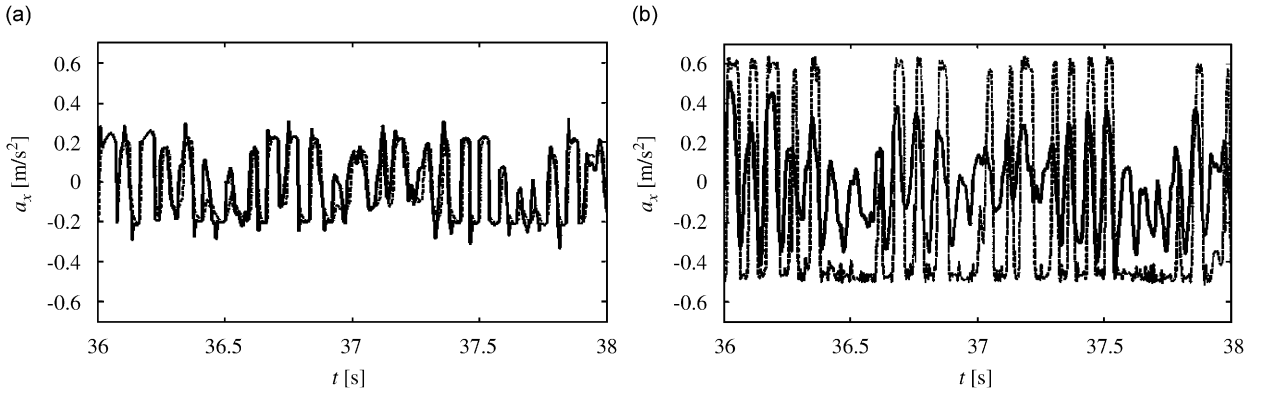

Fig. 15. Time histories of acceleration response for an oscillatory system with friction force under random excitation: (a) $F_{fk} = 15\,\mathrm{N}$, (b) $F_{fk} = 45\,\mathrm{N}$; stick–slip model (——), signum model (— —).

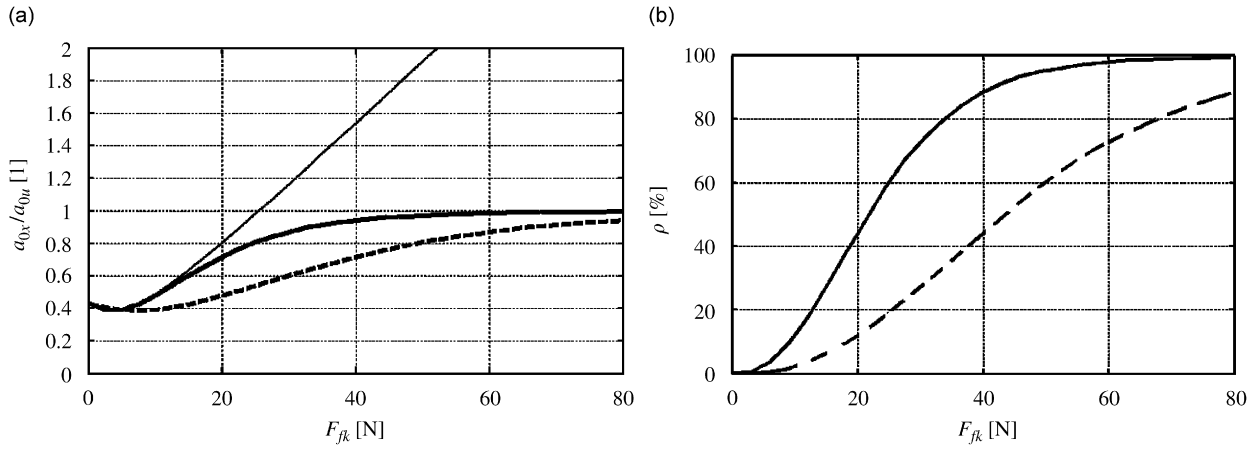

Fig. 16. (a) Acceleration transmissibility for the sdof oscillatory system with dry friction force under random excitation of two intensities, $a_{0u} = 0.33\,\mathrm{m\,s^{-2}}$ (——), $a_{0u} = 0.67\,\mathrm{m\,s^{-2}}$ (— —) and signum approach for $a_{0u} = 0.33\,\mathrm{m\,s^{-2}}$ (——); (b) corresponding incidence of sticking ρ.

calculated by the physically correct model at higher F_{fk} values, which results from the parasitic numerical oscillations. A similar response would be observed for the higher intensity excitation, but this has been omitted from the figure for clarity. Both courses start from the same point for $F_{fk} = 0$, which corresponds to the ratio a_{0x}/a_{0u} for a sdof oscillator without friction influence.

There is a difference in the system performance, depending on the excitation intensity. The transmissibility course for the lower intensity excitation approaches the asymptotic limit of unity at a lower dry friction force value, than does the course for the higher intensity. This is due to more frequent sticking, because the low intensity excitation at some time instants is not sufficient to excite the system beyond the adhesive force limit. This is also illustrated in the accompanying Fig. 16b, which shows the ratios ρ. Note that the eventual stopping of the oscillatory system with dry friction and consequently vibrating as a rigid body is not indicated by the frictionless sdof approach at all. Note that for low dry friction force values the sdof system with dry friction performs marginally better than the frictionless sdof system. The vibration attenuation is better by some 7.5%. The value of this minimum varies with the excitation and can be controlled to some extent by the dry friction force magnitude within a small band. This may be a way to improve performance of oscillatory systems provided that the friction magnitude can be adjusted in a controlled fashion.

As already noted, the ultimate test of each of the approaches is the comparison of simulation results with those measured in the field conditions. An oscillatory system of the same structure as used in the example; however, having slightly different parameters and substantially higher friction force, corresponding to that experimentally measured for a driver's seat horizontal suspension system [35] was subjected to acceleration excitation depicted in Fig. 14. An expanded time history segment of duration of 1.5 s of measured signal $a_x(t)$ on the isolated mass m (see Fig. 1b) is compared with the simulation result in Fig. 17. The signum approach was used in Fig. 17a, whereas the stick–slip approach was used in Fig. 17b. The match of the simulated output acceleration to that one measured in case sub (b) is self-evident and supports the hitherto described confidence in the developed friction force model and in the programme code used for simulation.

6. Dry friction force influence optimisation in a system without viscous damper

Having developed a physically correct simulation model of an oscillatory system with both viscous and dry friction dissipative terms, and noting some marginal improvement in vibration attenuation by adjustment of the dry friction force magnitude a question arises: Would it be possible for a system exposed to low magnitude random excitation, as sometimes experienced in ground transportation [35], to dispense of the viscous damper and rely fully on the dry friction for vibration energy dissipation? This approach could have some economic advantages.

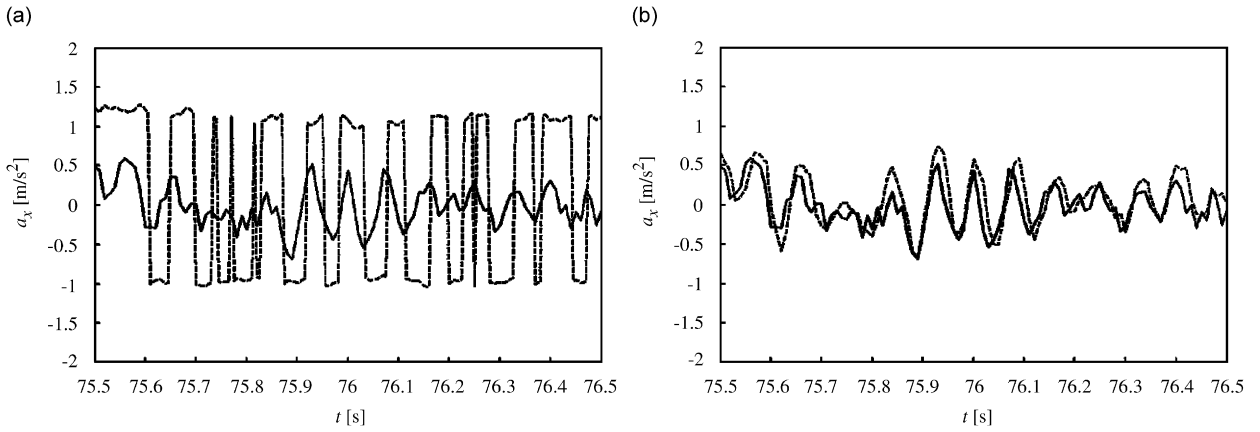

Fig. 17. Measured (——) and simulated (— —) time histories of acceleration response for real oscillatory system with friction force under random excitation: (a) signum model and (b) stick–slip model.

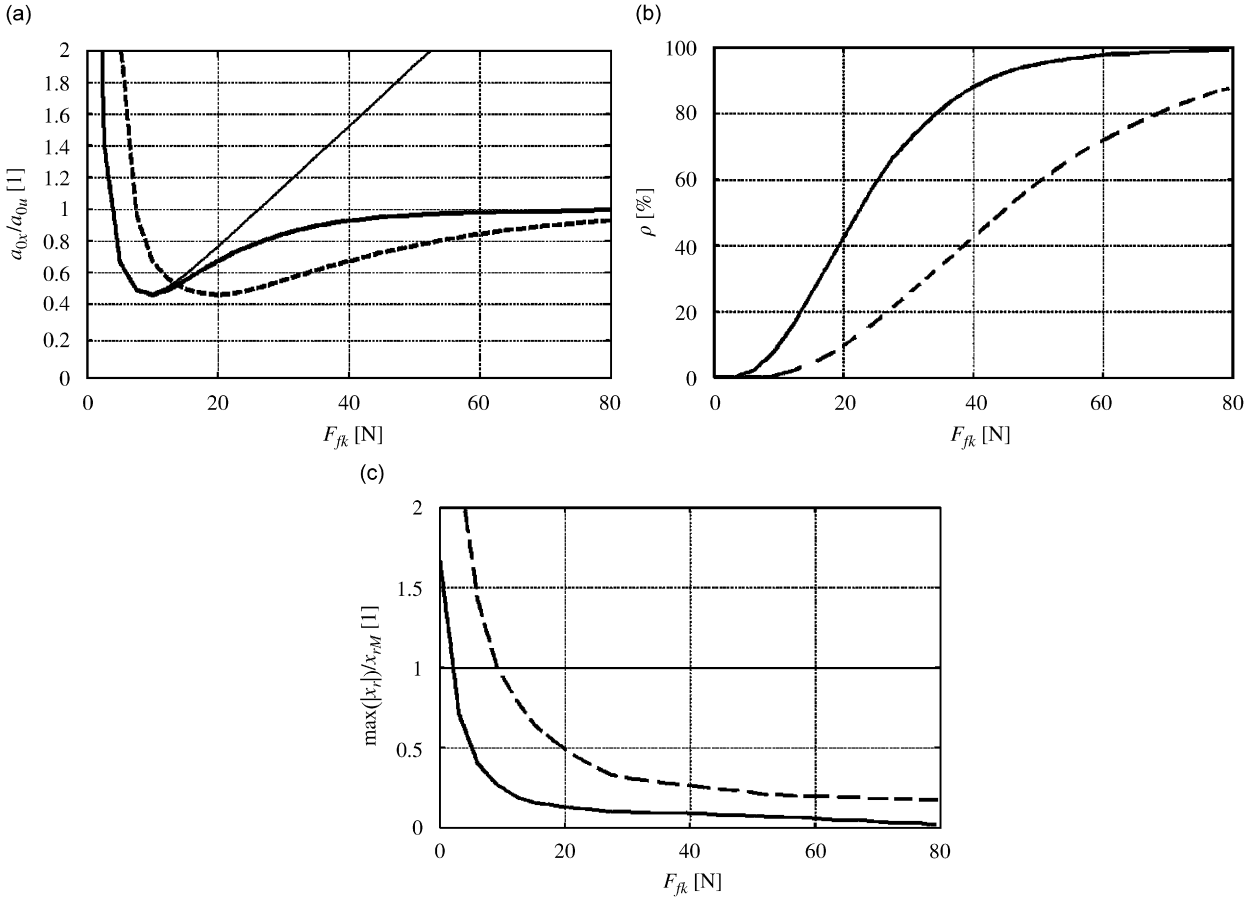

Fig. 18. (a) Acceleration transmissibility for the sdof oscillatory system with dry friction force only under random excitation with intensities, $a_{0u} = 0.33\,\mathrm{m\,s^{-2}}$ (——), $a_{0u} = 0.67\,\mathrm{m\,s^{-2}}$ (— —) and signum approach for $a_{0u} = 0.33\,\mathrm{m\,s^{-2}}$ (——); (b) corresponding incidence of sticking ρ; (c) absolute maximum values of x_r in comparison to x_{rM}.

In order to investigate this hypothesis, the model treated above and described by Eq. (13) was analysed once more, assuming $b = 0$. The equivalent curves to those of Fig. 16 were generated and are shown in Fig. 18, together with those for $\max(|x_r|)/x_{rM}$ as a test of consistency with the stroke limit. From inspection of Fig. 18a

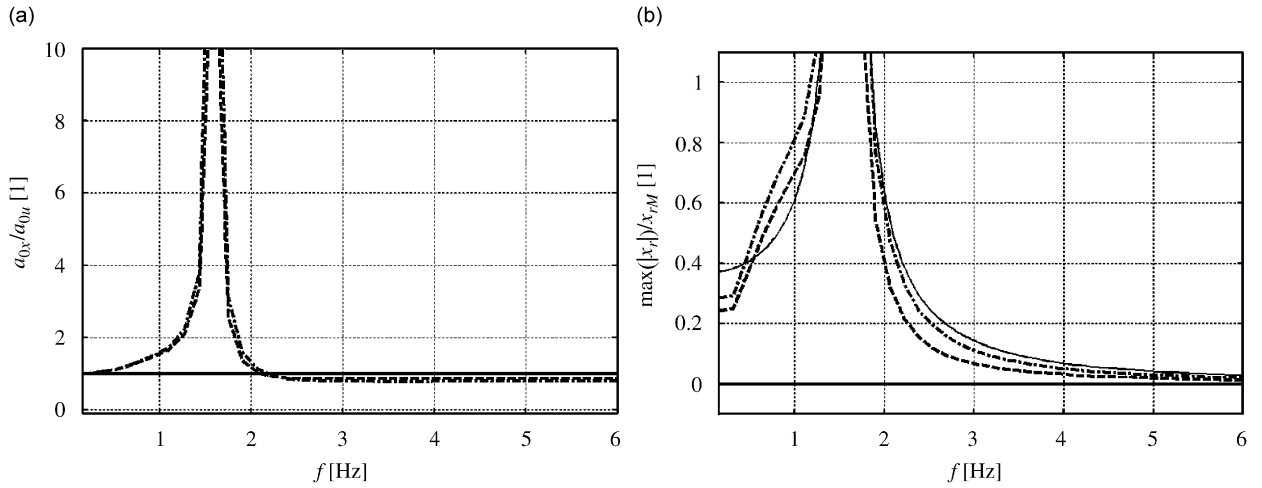

Fig. 19. Transfer function estimates for sdof oscillatory system with $F_{fk} = 45\,\mathrm{N}$ and without viscous damper for three excitation intensities $a_{0u} = 0.50\,\mathrm{m\,s^{-2}}$ (——), $0.67\,\mathrm{m\,s^{-2}}$ (— —), $0.75\,\mathrm{m\,s^{-2}}$ (— • —): (a) acceleration transmissibility and (b) absolute maximum values of x_r in comparison to x_{rM}.

it can be concluded that the course of both curves for $F_{fk} > 10\,\mathrm{N}$ and $F_{fk} > 20\,\mathrm{N}$ are very similar to those of Fig. 16a for a mixed damping oscillatory system. Also the courses of ratio ρ are nearly identical. The most important difference is for the dry friction force values below, say, 5–10 N, where the low friction is not sufficient to damp vibrations and the transmissibility exceeds reasonable limits. The stroke constraint x_{rM} is exceeded as the dry friction force decreases below some 10 N, as expected. A minimum in acceleration transmissibility is observable too, which is approximately coincident with the dry friction force values where the previous system exhibited a minimum.

A somewhat paradoxical, but important conclusion can be drawn—a sdof oscillatory system with an appropriate amount of dry friction can be subjected to low intensity random excitation, as occurring in some real situations, without deterioration in the acceleration attenuation and stroke control in comparison to a sdof system with both dry friction force *and* viscous damper. The system performance can be partially optimised, provided that the intensity of the random excitation is known beforehand and some means of dry friction force variation can be used, as described e.g. in Ref. [12]. However, *no viscous damper is really needed if shock-less excitation can be reasonably anticipated*.

This conclusion cannot be inferred from analysis of a sdof system with dry friction but *without* viscous damper if only harmonic analysis is used: The same system as described above was subjected to harmonic acceleration with RMS values of $a_{0u} = \{0.50, 0.67, 0.75\}\,\mathrm{m\,s^{-2}}$ and a dry friction force value $F_{fk} = 45\,\mathrm{N}$ with the results illustrated in Fig. 19. The steady-state responses are shown to exceed the stroke limit x_{rM} in the region of the resonance. For the lowest acceleration value $0.50\,\mathrm{m\,s^{-2}}$ ($K > 1$) the static force value of 52 N is not exceeded and hence the system is in a permanent standstill. Response for $a_{0u} = 0.75\,\mathrm{m\,s^{-2}}$, calculated according to the approximate formula Eq. (12b), following the Den Hartog's theory [3], is indicated in Fig. 19b by the thin line. Note the good approximation to the simulated response above resonance and in the vicinity of the resonance. For the sub-resonance region the approximation deteriorates due to the stops, which are not accounted for by the approximate analytical approach.

7. Conclusions

The paper deals with the analysis and simulation of a general sdof oscillatory system with vibratory energy dissipation by both an idealised linear viscous damper and a dry friction interface. For modelling of the dry friction interface the phenomenological approach is employed, described in mathematical form by the approximate harmonic balance approach, by the signum function approach and by the physically correct stick–slip approach, assuming switching phenomena within a short time scale. The differences in the last two

approaches are highlighted, indicating that the physically correct stick–slip approach describes the reality better than the simpler signum approach. The signum approach is prone to false numerical oscillations that completely distort the acceleration response signal. These effects are dependant on the relation between the dry friction force value, the isolated body equivalent excitation force (inertial force in the stick state) and the relative velocity between the sliding surfaces. This was illustrated on hand of comparison of field measurements and simulation results. The presented results give confidence in the developed stick–slip model code. Model analysis in respect to the friction force magnitude has been made, too.

It can be concluded that the simpler model, employing the signum function continuous approximation, is suitable for oscillatory systems with low inherent dry friction and high equivalent excitation force, whereas the limit force analysis approach is essential for correct modelling of systems with higher friction and low equivalent excitation force. The limit force analysis approach describes reality correctly from a physical point of view, including as it indeed does, also static friction. It is universally applicable for the modelling of any oscillatory system with dry friction in a generic way, irrespective of the magnitude of the Den Hartog's factor. It can accommodate also the cases with variable normal force, such as often encountered in practice, e.g. in transport industries. Its application circumvents the deeper knowledge of advanced methods of the nonlinear systems analysis and enables more effective exploitation of available simulation software for a better understanding of the performance of oscillatory systems.

A sdof oscillatory system without the viscous damper subjected to a stationary random acceleration and to a harmonic acceleration was analysed, too. It was shown that there is an important difference in the sdof oscillatory system with dry friction performance, if no viscous damper is installed when subjected to a stationary random excitation and stationary harmonic excitation with the same acceleration intensity. No inference from the system behaviour under steady harmonic excitation can be made in respect to the system behaviour under random excitation. There are even some limited real life cases, occurring in the transport industries, when the dry friction damping is sufficient and sometimes slightly more effective than a viscous damper.

Acknowledgement

This paper was prepared within the Project no. 2/6161/26 of the Slovak VEGA Grant Agency for Science. The paper is based on data and experience from laboratory and field measurements obtained within the European research project VIBSEAT (Contract no. GR3D-CT-2002-00827 of the European Commission). The support of both Agencies is gratefully acknowledged. Authors are also indebted to Mr. Richard Stayner of RMS Vibration, UK for valuable discussions and comments.

References

[1] E.J. Berger, Friction modeling for dynamic system simulation, *Applied Mechanics Reviews* 55 (2002) 535–577.
[2] J.P. Den Hartog, Forced vibrations with combined coulomb and viscous friction, *Transaction of the ASME* 53 (1931) 107–115.
[3] F. Pfeiffer, Dynamical systems with time-varying or unsteady structure, *ZAMM-Zeitschrift für angewandte Mathematik und Mechanik* 71 (1991) 6–22.
[4] J.H. Taylor, Modelling and simulation of dynamic systems – a tutorial, *Proceedings of the M^2SABI'01 Conference*, Haifa, Israel, 2001.
[5] K. Popp, L. Panning, W. Sextro, Vibration damping by friction forces: theory and applications, *Journal of Vibration and Control* 9 (2003) 419–448.
[6] K. Klotter, *Technische Schwingungslehre, Teil B*, Springer, Berlin, Germany, 1980.
[7] E. Marui, S. Kato, Forced vibration of a base-excited single-degree-of-freedom system with coulomb friction, *Journal of Dynamical Systems Measurement and Control* 106 (1984) 280–285.
[8] R.I. Leine, D.H. van Campen, Discontinuous fold bifurcation in mechanical systems, *Archives of Applied Mechanics* 72 (2001) 138–146.
[9] I. López, J.M. Busturia, H. Nijmeijer, Energy dissipation of a friction damper, *Journal of Sound and Vibration* 278 (2003) 539–561.
[10] M.S. Hundal, Response of base-excited system with Coulomb and viscous friction, *Journal of Sound and Vibration* 64 (1979) 371–378.
[11] A. Schlesinger, Vibration isolation in the presence of Coulomb friction, *Journal of Sound and Vibration* 63 (2) (1979) 213–224.
[12] C.W. Stammers, T. Sireteanu, Vibration control of machines by use of semi-active friction damping, *Journal of Sound and Vibration* 209 (4) (1998) 671–684.
[13] R. Brepta, L. Půst, F. Turek, *Mechanické kmitání*, Sobotales, Prague, Czech Republic, 1994 (in Czech).

[14] S. Timoshenko, D.H. Young, W. Weaver Jr., *Vibration Problems in Engineering*, Wiley, New York, 1974.
[15] P. Wriggers, U. Nackenhorst (Eds.), *Analysis and Simulation of Contact Problems. Lecture Notes in Applied and Computational mechanics*, Vol. 27, Springer, Berlin, Heidelberg, Germany, 2006.
[16] S. Rakheja, Y. Afework, S. Sankar, An analytical and experimental investigation of the driver-seat-suspension system, *Vehicle System Dynamics* 23 (7) (1994) 501–524.
[17] T.P. Gunston, VIBSEAT project internal Technical Report, ISVR, Southampton 2005.
[18] T.P. Gunston, J. Rebelle, M.J. Griffin, A comparison of two methods of simulating seat suspension dynamic performance, *Journal of Sound and Vibration* 278 (1−2) (2004) 117–134.
[19] B. Fenny, A. Guran, N. Hinrichs, K. Popp, A historical review on dry-friction and stick–slip phenomena, *Applied Mechanics Review* 51 (1998) 321–341.
[20] E.P. Petrov, D.J. Ewins, Models of friction damping with variable normal load for time-domain analysis of vibrations, *Proceedings of the ISMA 2002 Conference*, Leuven, Belgium, 2002, pp. 421–430.
[21] N. Andreaus, P. Casini, Dynamics of friction oscillators excited by a moving base and/or driving force, *Journal of Sound and Vibration* 245 (2001) 685–699.
[22] A. Al Majid, R. Dufour, Formulation of a hysteresis restoring force model. Application to vibration isolation, *Nonlinear Dynamics* 27 (2002) 69–85.
[23] A. Al Majid, R. Dufour, Harmonic response of a structure mounted on an isolator modelled with a hysteretic operator: experiments and prediction, *Journal of Sound and Vibration* 227 (2004) 391–403.
[24] J. Bastien, G. Michon, L. Manin, R. Dufour, An analysis of the modified Dahl and Masing models: application to a belt tensioner, *Journal of Sound and Vibration* 302 (4–5) (2007) 841–864.
[25] N. Mostaghel, T. Davis, Representations of Coulomb friction for dynamic analysis, *Earthquake Engineering and Structural Dynamics* 26 (1997) 541–548.
[26] L. Ljung, T. Glad, *Modelling of Dynamical Systems*, Prentice-Hall Inc., Englewood Cliffs, NJ, 1994.
[27] R. Zahoranský, G.J. Stein, H. Meyer, Modelling and simulation of kinematically excited vibration isolation systems with friction, under random and harmonic excitation, *Proceedings of the European Non-linear Conference*, Eindhoven, the Netherlands, 2005, pp. 2663–2671.
[28] A. Trontis, G. Pasgianos, A.K. Boglou, K. Arvanitis, Stabilization and dynamic friction compensation for the inverted pendulum via the backstepping technique, *Proceedings of the MECH2K4 Conference*, Prague, Czech Republic, 2004.
[29] D. Karnopp, Computer simulation of stick–slip friction in mechanical dynamical systems, *Journal of Dynamical Systems Measurement and Control* 107 (1985) 100–103.
[30] D.J. Inman, *Engineering Vibration*, second ed., Prentice-Hall Inc., Upper Saddle River, NJ, USA, 2001.
[31] I. Dobiáš, *Nelineární dynamické soustavy s náhodnými vstupy*, Academia, Prague, Czech Republic, 1988 (in Czech).
[32] D. Capecchi, F. Vestroni, Periodic response of a class of hysteretic oscillators, *International Journal of Non-Linear Mechanics* 25 (2–3) (1990) 309–317.
[33] Using MATLAB®, Version 6, The MathWorks Inc., Natick, MA, 2000.
[34] N. Mostaghel, A non-standard analysis approach to systems involving friction, *Journal of Sound and Vibration* 284 (2005) 583–595.
[35] G.J. Stein, R. Zahoranský, P. Múčka, R. Chmúrny, H. Mayer, On dry-friction modelling in simple, kinematically excited, vibration isolation systems, *Proceedings of the ISMA 2004 Conference*, Leuven, Belgium, 2004, pp. 649–663.